NOTATION

a_c, a_p = collector radius and particle radius
A = control surface area
b_i = coefficients of Equation (8)
c = particle concentration
C = Cunningham correction factor
E = efficiency defined by Equation (4)
f_1, f_2 = parametric functions representing particle trajectory
i, j = indexes of sequences
M = total number of particles considered
m = total number of particles collected among M particles considered
N_R = relative size parameter defined as the ratio of particle radius to collection radius a_p/a_c
N_{St} = Stokes number defined as $2C\rho_p V a_p^2/9\mu a_c$
N = number of particles passing through the control surface
r = radial distance
$\overline{r_i}$ = position of i^{th} deposited particle
Δt = time interval
t = time
V = approaching velocity
W = deposition rate over a collector
X = lateral position from the center axis
X_o = maximum lateral distance from the center axis on the control surface
X_{cr} = distance between the limiting trajectory and central axis upstream
$(X_{cr})_o$ = values of X_{cr} corresponding to a clean collector
η = collection efficiency
θ = angular position
μ = viscosity of fluid media
ρ_p = density of particle

LITERATURE CITED

Albrecht, F., "Theoretische Untersuchungen uber die Ablagerung von Staub aus stromender Luft und ihre Anwendung auf die Theorie der Staubfilter," *Phys. Z.*, **32**, 48 (1931).

Beizaie, Masoud, "Deposition of Particles on a Single Collector," Ph.D. dissertation, Chemical Engineering, Syracuse Univ., N.Y. (1977).

Billings, C. E., "Effect of Particle Accumulation in Aerosol Filtration," Ph.D. dissertation, Calif. Int. Tech., Pasadena (1966).

Bosanquet, C. H., "Impingment of Particles on Obstacles in a Stream," appendix "Dust Collection by Impingement and Diffusion," C. J. Stairmand, *Trans. Inst. Chem. Engr. (London)*, **28**, 130 (1950).

Clarenburg, L. A., and R. M. Werner, "Aerosol Filters," *Ind. Eng. Chem. Process Design Develop.*, **4**, 293 (1965).

Davies, C. N., *Air Filtration*, Academic Press, New York (1973).

Green, H. L., *Phil. Mag.*, **4**, 1046 (1927) as quoted in *Particulate Clouds—Dust Smokds and Mists*, H. L. Green, and W. R. Lane, p. 281, Van Nostrand, New York (1964).

Hutchison, H. P., and D. N. Sutherland, "An Open-Structured Random Solid," *Nature*, **206**, 1036 (1965).

Ives, K. J., "Theory of Filtration," Special Subject No. 7, Int'l Water Supply Congress and Exhibition, Vienna (1969).

Langmuir, I., and K. B. Blodgett, "Mathematical Investigation of Water Droplet Trajectories," *Rept. No. R.L. 225*, General Electric Research Laboratory, Schenectady, New York (1944-1945).

Moshman, J., "Random Number Generation," in *Mathematical Methods for Digital Computers*, Vol. 2, p. 4, Anthony Ralston and Herbert S. Wilf., ed., Wiley. New York (1967).

Payatakes, A. C., Chi Tien, and R. M. Turian, "Trajectory Calculation of Particle Deposition in Deep Bed Filtration, I: Mode Formulation, II Case Study," *AIChE J.*, **20**, 889,905 (1974).

Payatakes, A. C., and Chi Tien, "Particle Deposition in Fibrous Media with Dendrite-like Pattern; A Preliminary Model," *J. Aerosol Sci.*, **7**, 85, (1976).

———, "Model of Transient Aerosol Particle Deposition in Fibrous Media with Dendritic Pattern," *AIChE J.*, **23**, 192 (1977).

Rajagopalan, R., and Chi Tien, "Trajectory Analysis of Deep Bed Filtration with Sphere-in-Cell Porous Media Model," *ibid.*, **22**, 523 (1976).

Sell, W., "Staubausscheidung an einfachen Koerpern und in Luftfiltern," *Ver. Deut. Ing. Forschungshaft*, No. 347 (1931).

Speilman, L. A., and J. A. Fitzpatrick, "Theory of Particle Collection Under London and Gravity Forces," *J. Coll. Interface Sci.*, **42**, 607 (1973).

Tien, Chi, Chiu-sen Wang, and D. T. Barot, "Chain-like Formation of Particle Deposits in Fluid Particle Separation," *Science*, **196**, 983 (1977).

Yao, K. M., M. T. Habibian, and C. R. O'Melia, "Water and Waste Water Filtration Concepts and Application," *Environ. Sci. Technol.*, **5**, 1105 (1971).

Manuscript received September 2, 1976; revision received August 1, and accepted August 9, 1977.

Experimental Study of Eddy Diffusion Model for Heated Turbulent Free Jets

KUNIO KATAOKA

and

TOHRU TAKAMI

Department of Chemical Engineering
Kobe University
Rokko, Kobe 657
Japan

Prandtl's eddy diffusion model was successfully extended to turbulent momentum, energy, and mass transfer in nonisothermal free jets by taking into account the effect of change in volume of traveling eddies. The present model was experimentally confirmed for the high temperature, low velocity, turbulent free jets produced by combustion of methane gas.

SCOPE

Problems of heat and mass transfer in impinging jets have recently led to a need for information that will permit accurate prediction of the temperature, velocity, and concentration fields at various temperature levels. From an engineering viewpoint, these problems become very important, especially when a nonisothermal free jet

Correspondence concerning this paper should be addressed to Kunio Kataoka.

impinges on a heat transfer surface, such as in heating, drying, and melting technology. The present study is concerned with an eddy diffusion model of the turbulent transport in nonisothermal free jets of heated gas as the first phase of an investigation of nonisothermal impinging jets. Although considerable experimental data are available for isothermal (or incompressible) free jets, very little work has been done at high temperatures. When a high temperature free jet issues from a nozzle into the quiescent ambient fluid at a low temperature, physical properties will also change greatly in the flow field owing to large temperature differences between the jet and the ambient. There are several theoretical methods to the problem of solving for the velocity, temperature, and concentration of nonisothermal, heated jets as a function of position. However, all these techniques depend ultimately on various simplifying assumptions based on the experimental turbulent mixing data, since an essential part of all these techniques is the specification of local eddy diffusivities in the particular jet flow in question. Therefore, it is necessary to extend Prandtl's eddy diffusivity model to the gas flow field with large thermal gradients. The objective of the present study is to measure the local variation of eddy diffusivities in the turbulent free jets of heated gas and to obtain experimentally a universal eddy diffusion model which holds in the fully developed region over the wide range of the initial temperature ratio, that is, of the ratio of the jet temperature at a nozzle exit to the ambient temperature.

CONCLUSIONS AND SIGNIFICANCE

Prandtl's eddy diffusivity model was successfully extended to turbulent momentum, energy, and mass transfer in nonisothermal, low velocity, turbulent free jets by taking into account the change in volume of traveling eddies with temperature. The model based on the dynamic eddy transfer coefficients was experimentally confirmed to be useful in the fully developed region for nonisothermal, heated jets at various initial temperature ratios as well as for isothermal (or incompressible) jets. The observed dynamic eddy transfer coefficients, as do the eddy diffusivities in the case of isothermal jet, remain almost constant over the fully developed region of heated jets, where the effect of free convection can be neglected. The values obtained by applying the present model to the isothermal condition agree well with the eddy diffusivity data for isothermal jets given in the literature.

PREVIOUS WORK

Corrsin and Uberoi (1949) obtained experimental data for elevated temperature (up to 385°C), low Mach number air jets and found the turbulent Prandtl number to be 0.74, the same as the Prandtl number for molecular transport.

Hinze and van der Hegge Zijnen (1949) obtained not only a similar turbulent Prandtl number on jets of air, but also a turbulent Schmidt number of 0.74.

Kiser (1963) reported similar measurements on liquid jets by using a jet of the dilute solution of sodium chloride. However, these investigations did not need to take into account the effect of change in volume of traveling eddies on the eddy diffusivity model because of the zero or small temperature differences in the flow field.

Warren (1957) performed a number of experiments on the mixing of compressible heated jets and analyzed the results with the aid of the momentum integral method. The mixing rate parameter was found to be only a function of the Mach number at the nozzle exit.

Ferri et al. (1962) tried to formulate the eddy viscosity for compressible jets in terms of compressible flow variables and an arbitrary constant to be determined experimentally.

Kleinstein (1964) obtained solutions for the velocity, temperature, and concentration profiles in the fully developed region by the linearization of the conservation equations in the plane of von Mises variables. A dynamic eddy transfer coefficient $\rho\epsilon_M$ due to Ferri et al. was considered to be more suitable than Prandtl's eddy diffusivity ϵ_M as a measure of the turbulent diffusion phenomena for compressible flows.

Donaldson and Gray (1966) developed a model for predicting the turbulent mixing of dissimilar gases with an extension of Warren's momentum integral method. They found the mixing rate parameter to be only a function of a suitably chosen local Mach number.

O'Connor et al. (1966) determined experimentally the radial and axial variation of velocity, enthalpy, and con-

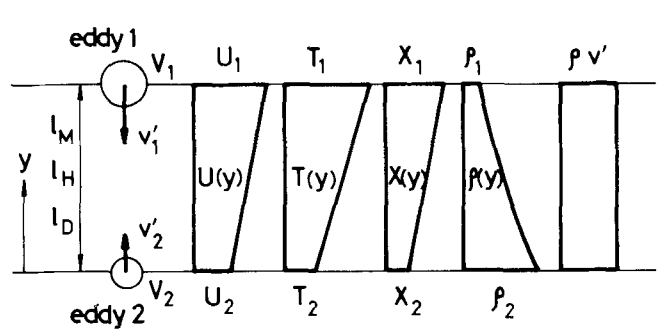

Fig. 1. Dynamic eddy diffusion model for turbulent transport of momentum, heat, and mass in gas flows with large thermal gradients.

centration in the high temperature (5 800°K), compressible jets of partially dissociated nitrogen.

Tomich and Weger (1967) investigated both experimentally and theoretically a relatively high initial temperature (700°C) jet at high subsonic Mach numbers. They obtained solutions by means of a finite-difference technique with the modification of Kleinstein's compressible formulation of the eddy viscosity.

Stowell and Smoot (1973) obtained a correlative form of the turbulent mixing coefficients.

Witze (1974) presented a theory applicable to the main region of most classes of free jets by introducing an empirically determined formulation for the eddy viscosity into the Kleinstein's theory.

Still, the accurate representation of the local eddy diffusivities for highly heated jets has not been satisfactorily completed. The present investigation is a continuation of those due to Kleinstein, Tomich and Weger, and Witze.

EDDY DIFFUSION MODEL

Prandtl's eddy diffusivity model for incompressible flows can be extended to nonisothermal turbulent free jets of heated gas at low Mach numbers by taking into account only the change in volume of traveling eddies due to the large thermal gradients.

Consider two eddies, as shown in Figure 1, in the gas flow field with large thermal gradients, which are exchanged over the so-called mixing length (l_M, l_H, l_D) in the transverse direction with conservation of their original quantities, that is, (U_1, T_1, X_1, ρ_1) and (U_2, T_2, X_2, ρ_2). It can be considered that the volume V of the traveling eddy transported per unit area and unit time is proportional to the transverse component of turbulent velocity v'. Hence

$$\rho_1 v_1' = \rho_2 v_2' = \rho v' = \text{constant} \qquad (1)$$

everywhere in the transverse direction. This static pressure and the heat capacity of gas are also assumed to be constant in the model consideration.

The turbulent fluxes of momentum, heat, and mass resulting from the exchange of the two eddies can be written as

$$\left\{\begin{aligned}
\tau_t &= \rho_2 U_2 v_2' - \rho_1 U_1 v_1' = \rho v'(U_2 - U_1) \\
&= \rho v' l_M \frac{dU}{dy} = \rho \epsilon_M \frac{dU}{dy} \\
q_t &= \rho_2 C p_2 T_2 v_2' - \rho_1 C p_1 T_1 v_1' = \rho v' C p (T_2 - T_1) \\
&= \rho C p v' l_H \frac{dT}{dy} = \rho C p \epsilon_H \frac{dT}{dy} \\
j_t &= \rho_2 (X_2/M_2) v_2' - \rho_1 (X_1/M_1) v_1' \\
&= \rho v' ((X_2/M_2) - (X_1/M_1)) \\
&= \rho v' l_D \frac{d(X/M)}{dy} = \rho \epsilon_D \frac{d(X/M)}{dy}
\end{aligned}\right. \qquad (2)$$

These expressions are similar in form to those for incompressible flows, but they suggest that the turbulent, gradient transport model for nonisothermal, heated jets should be discussed in terms of Kleinstein's type of dynamic eddy transfer coefficient $\rho\epsilon_M$ rather than the Prandtl's eddy diffusivity ϵ_M.

Figure 2 shows the flow configuration of interest and the coordinate system. The problems of momentum, heat, and mass transfer in free jets are, in general, of a boundary-layer nature. Purely laminar effects can be neglected with

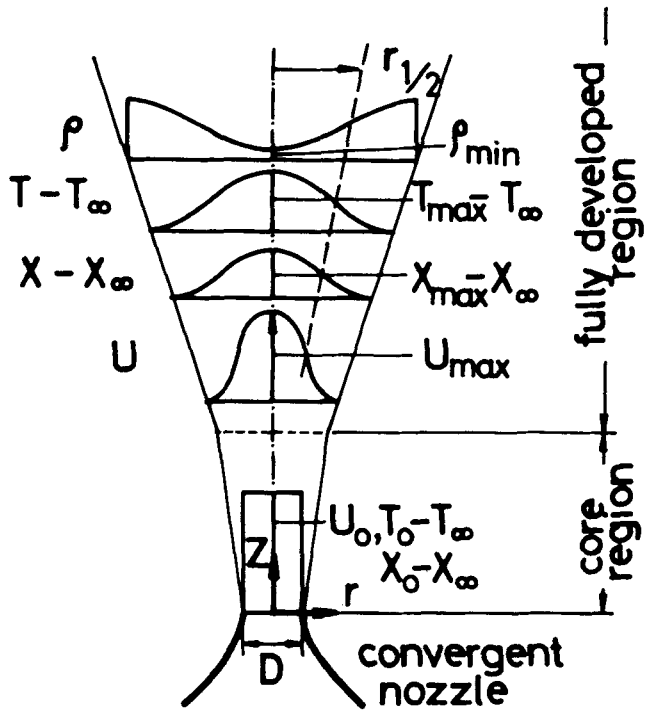

Fig. 2. Flow configuration of axisymmetric, turbulent free jets of heated gas and the coordinate system.

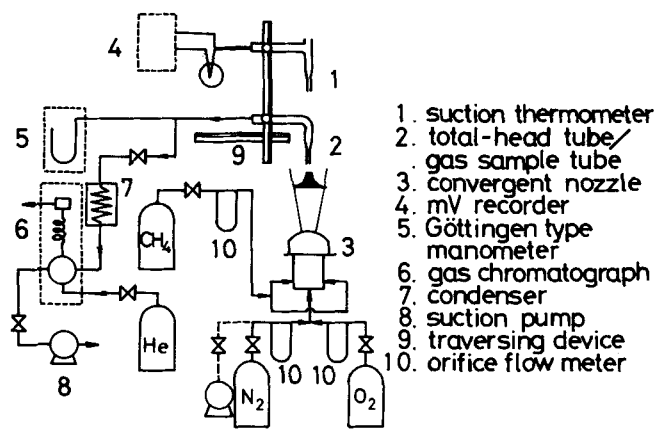

Fig. 3. General arrangement of the apparatus.

respect to the turbulent effects for turbulent jets. Consideration is restricted to the case of very low Mach numbers. The boundary-layer equation for axisymmetric jets are

$$\left\{\begin{aligned}
&\frac{\partial}{\partial Z}(\rho U) + \frac{1}{r}\frac{\partial}{\partial r}(\rho r V) = 0 \\
&\rho U \frac{\partial U}{\partial Z} + \rho V \frac{\partial U}{\partial r} = \frac{1}{r}\frac{\partial}{\partial r}\left(\rho \epsilon_M r \frac{\partial U}{\partial r}\right) \\
&\rho C p U \frac{\partial T}{\partial Z} + \rho C p V \frac{\partial T}{\partial r} = \frac{1}{r}\frac{\partial}{\partial r}\left(\rho C p \epsilon_H r \frac{\partial T}{\partial r}\right) \\
&\rho U \frac{\partial (X/M)}{\partial Z} + \rho V \frac{\partial (X/M)}{\partial r} \\
&\qquad = \frac{1}{r}\frac{\partial}{\partial r}\left(\rho \epsilon_D r \frac{\partial (X/M)}{\partial r}\right)
\end{aligned}\right. \qquad (3)$$

where buoyancy forces have been neglected. All densities, velocities, temperatures, and concentrations have been

time smoothed for turbulent flow. When these relations are integrated over the transverse coordinate with the aid of the continuity equation, the following expressions for the eddy diffusivities are obtained:

$$\left\{\begin{aligned}
\epsilon_M &= \frac{1}{\rho r \dfrac{\partial U}{\partial r}} \int_0^r \left[r\rho U \frac{\partial U}{\partial Z} - \frac{\partial U}{\partial r} \int_0^r r \frac{\partial}{\partial Z}(\rho U)\,dr \right] dr \\
\epsilon_H &= \frac{1}{\rho Cpr \dfrac{\partial T}{\partial r}} \int_0^r \left[r\rho CpU \frac{\partial T}{\partial Z} - Cp \frac{\partial T}{\partial r} \int_0^r r \frac{\partial}{\partial Z}(\rho U)\,dr \right] dr \\
\epsilon_D &= \frac{1}{\rho r \dfrac{\partial (X/M)}{\partial r}} \int_0^r \left[r\rho U \frac{\partial (X/M)}{\partial Z} - \frac{\partial (X/M)}{\partial r} \int_0^r r \frac{\partial}{\partial Z}(\rho U)\,dr \right] dr
\end{aligned}\right. \tag{4}$$

The right-hand sides of Equation (4) are numerically integrated to calculate the local eddy diffusivities with the aid of the observed axial and radial distributions of axial velocity, temperature, and concentration.

EXPERIMENTAL

The experimental apparatus is shown schematically in Figure 3. It consisted of a stainless steel nozzle assembly which provided high temperature free jets by combustion of methane gas and a measuring system with the traversing device for three types of probes.

The nozzle assembly, as shown in Figure 4, consisted of a burner with a venturi type of throat for intimately mixing methane gas with an oxidizing stream, a 40 mm ID combustion chamber with a straight section 100 mm long, and a 10 mm ID convergent nozzle with a contraction ratio 1/16. The combustion chamber and the convergent nozzle section were joined by smooth curved surfaces to provide as low initial turbulence jets as possible. The nozzle outlet was also arranged flush with, and central to, the horizontal surface of an insulating firebrick not only to provide as uniform initial temperature profiles as possible, but also to prevent entrainment of the ambient air from behind the nozzle. (This nozzle can be regarded as the so-called blunt edged nozzle classified by Donaldson and Gray). Oxygen was mixed with nitrogen so as not to damage the wall of the convergent nozzle owing to high temperature and admitted to the burner section of the nozzle assembly as the oxidizer. Methane gas was emitted into the oxidizing stream from two 6 mm ID holes drilled in the wall of the throat section. At first, a small amount of the enriched combustible mixture was ignited at the exit of the convergent nozzle. Then the flame was carried back into the combustion chamber by increasing the oxygen concentration. The methane, oxygen, and nitrogen flows were separately regulated with a needle type of flow controller to maintain the accurate jet conditions. Thereafter, the ratio of the molar flow rates was kept CH_4:O_2:N_2 = 1:3.3:5.2 to make the nitrogen/oxygen ratio of the burned gas equal to that of the ambient air. The hot jet produced by combustion of methane gas was exhausted vertically upward into the quiescent ambient air at room temperature. Although the excess oxidizer was supplied for complete combustion, the percentage of the reaction completed was measured by a composition analysis of the gas sample taken at the nozzle exit. It was confirmed that no

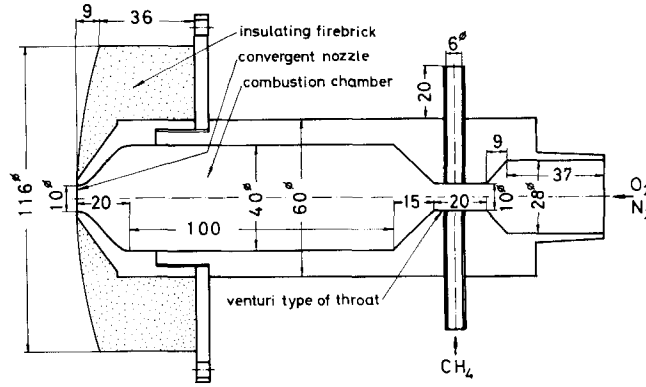

Fig. 4. Circular convergent nozzle having a combustion chamber. Dimensions given are in millimeters.

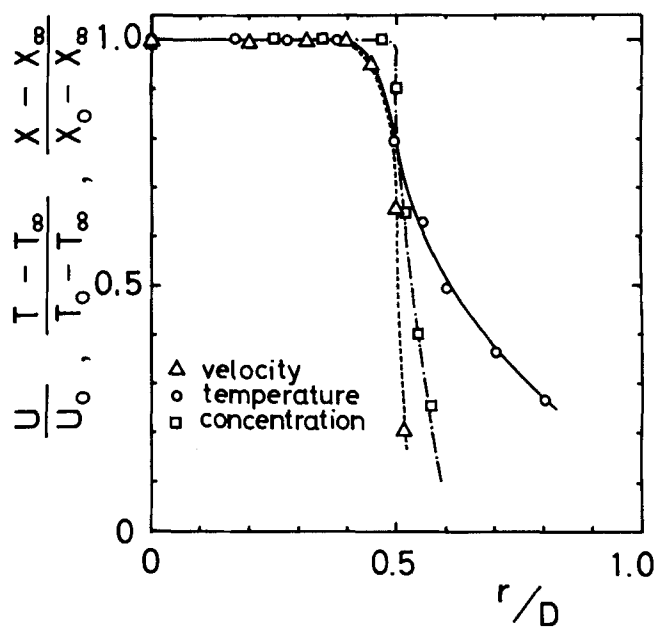

Fig. 5. Initial radial profiles of velocity, temperature, and concentration.

burning mixture issued from the nozzle. The average molecular weight of the burned gas was also nearly equal to that of air. For simplicity, the physical properties were determined from those of air. However, the error was negligibly small in the fully developed region.

The effect of free convection due to the large temperature differences between the jet and the ambient was considered to be negligibly small because $Gr/Re^2 = 2.0 \times 10^{-4}$ at the nozzle exit ($Z/D = 0$) and $Gr/Re^2 = 5.8 \times 10^{-3}$ at $Z/D = 20$, where the jet half radii $r_{1/2T}$, $r_{1/2U}$, the temperature difference $T_{max} - T_\infty$, and the center line velocity U_{max} were used as the characteristic length, temperature difference, and velocity, respectively. The effect of compression due to the velocity changes was also considered to be negligibly small because $Ec = 2.9 \times 10^{-5}$ at $Z/D = 0$ and $Ec = 1.4 \times 10^{-6}$ at $Z/D = 20$.

The gas temperature was measured directly by a suction thermometer of 0.2 mm diameter Pt-PtRh thermocouple, which was protected from radiation by a 1.2 mm OD opaque quartz tube. The measured radiation error was found to be of the order 1%. The velocity was calculated with the aid of the observed gas temperature from the dynamic pressure measured by a miniature pitot tube of 1.4 mm OD quartz tube, which also served as a sampling probe. The gas composition was determined in terms of the carbon dioxide-air mole fraction measured by means of gas chromatograph. The thermal

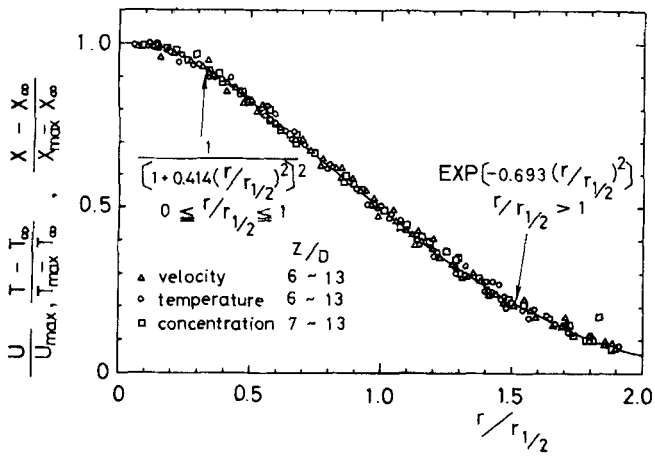

Fig. 6. Normalized radial distributions in the fully developed region.

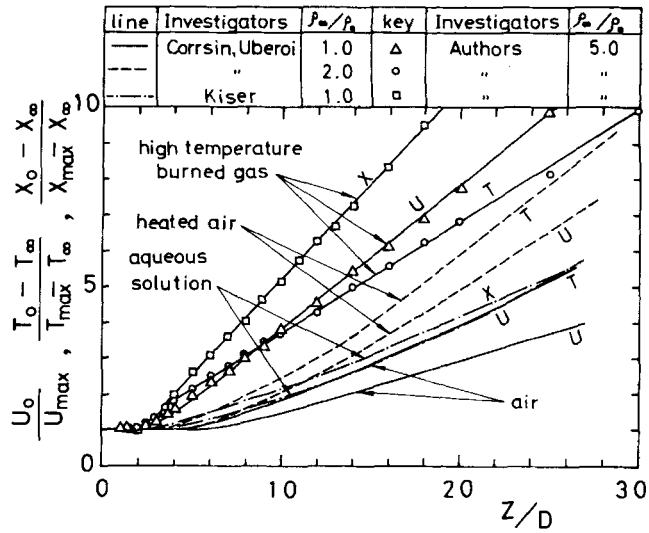

Fig. 7. Axial decay of center-line velocity, temperature, and concentration. (The solid lines connecting experimental data points are only for clarification of the linear variation.)

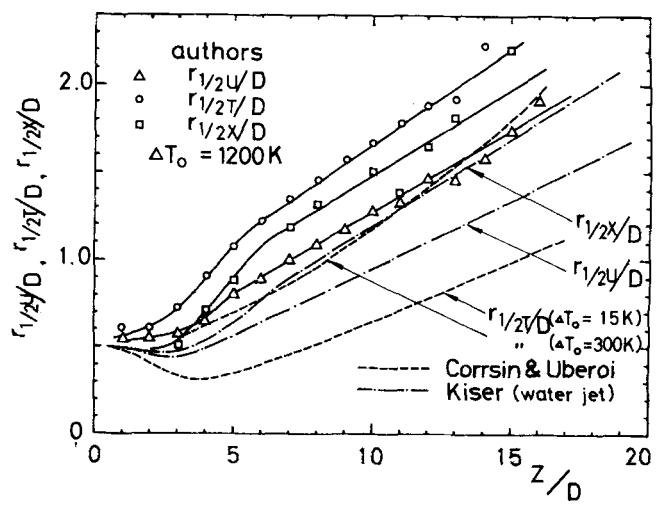

Fig. 8. Radial spreading of velocity, temperature, and concentration. (The solid lines connecting experimental data points are only for clarification of the linear variation.)

conductivity cell was calibrated with known prepared gas samples of varying carbon dioxide-air fraction. The gas sample of the burned gas jets was sucked through the miniature pitot tube with the same velocity as that of the flow field. A condenser was placed between the probe and the valve in the sampling line, which allowed only the condensible component water to be removed from the gas sample. These probes were able to move to any position by means of the traversing device with accurate lead screws that allowed their locations to be determined with an accuracy of 0.1 mm or better. Measurements of the radial and axial property variations were made every 1 mm in the radial direction and every 10 mm in the axial direction, mainly in the fully developed region.

The experimental conditions were limited to an unexpectedly narrow range to maintain the flame stability of the burner. Only one experiment was conducted elaborately at the most stable condition to obtain accurate variations of the local eddy diffusivities.

Experimental conditions are initial velocity $U_o = 34$ m/s, initial temperature $T_o = 1\,593$°K, ambient temperature $T_\infty = 293$°K, initial concentration $X_o = 0.098$, ambient concentration $X_\infty = 0.00024$, exit Reynolds number $Re_o = U_oD/\nu_o = 1\,350$, initial density ratio $\rho_\infty/\rho_o = 5.10$, initial temperature ratio $T_o/T_\infty = \rho_\infty/\rho_o = 5.10$, and Prandtl number at the nozzle exit $Pr_o = 0.68$.

Three other supplementary experiments were performed only for spot checks of the experimental results of the dynamic eddy transfer coefficient for momentum at $Re_o = 1600$ in the range of $T_o/T_\infty = 3.1$ to 5.1.

EXPERIMENTAL RESULTS AND DISCUSSION

The initial radial profiles taken just downstream of the nozzle exit ($Z/D = 0.1$) are shown in Figure 5. The uniform distribution has been confirmed for about 90% of the 10 mm diameter.

The normalized radial distributions of jet velocity, temperature, and concentration in the fully developed region are shown in Figure 6. The center-line decay and the radial spreading are also shown in Figures 7 and 8. As is evident from these figures, the highly heated jets still exhibit turbulent mixing characteristics similar to those of unheated (or incompressible) jets in the fully developed region ($Z/D \geqq 6$). The radial profiles are similar at various axial positions and can be well described by the theoretical curves given by the isothermal analysis in the literature. The center-line quantities (U_{max}, $T_{max} - T_\infty$, $X_{max} - X_\infty$) decrease linearly, whereas the jet half radii ($r_{1/2U}$, $r_{1/2T}$, $r_{1/2X}$) increase linearly with increasing axial distance. The best fit curve connecting the experimental data points in Figure 6 can be expressed by Equation (5) in the inner jet region ($0 \leqq r/r_{1/2} \leqq 1$) and by Equation (6) in the outer, intermittent region ($r/r_{1/2} > 1$), respectively:

$$\begin{cases} \dfrac{U}{U_{max}} = \dfrac{1}{[1 + 0.414\,(r/r_{1/2U})^2]^2} \\ \dfrac{T - T_\infty}{T_{max} - T_\infty} = \dfrac{1}{[1 + 0.414\,(r/r_{1/2T})^2]^2} \\ \qquad\qquad (0 \leqq r/r_{1/2} \leqq 1) \quad (5) \\ \dfrac{X - X_\infty}{X_{max} - X_\infty} = \dfrac{1}{[1 + 0.414\,(r/r_{1/2X})^2]^2} \end{cases}$$

$$\begin{cases} \dfrac{U}{U_{max}} = \mathrm{EXP}\,[-0.693\,(r/r_{1/2U})^2] \\ \dfrac{T - T_\infty}{T_{max} - T_\infty} = \mathrm{EXP}\,[-0.693\,(r/r_{1/2T})^2] \\ \qquad\qquad (r/r_{1/2} > 1) \quad (6) \\ \dfrac{X - X_\infty}{X_{max} - X_\infty} = \mathrm{EXP}\,[-0.693\,(r/r_{1/2X})^2] \end{cases}$$

These equations are mathematically similar to those for the isothermal jet, except in that the half radii of nonisothermal jets are used as the characteristic jet width; Equation (5) is similar in form to the theoretical solution for

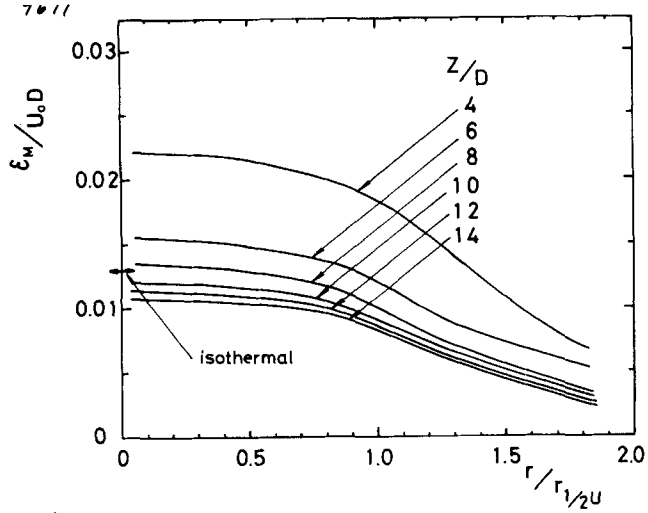

Fig. 9. Radial distribution of eddy diffusivity for momentum.

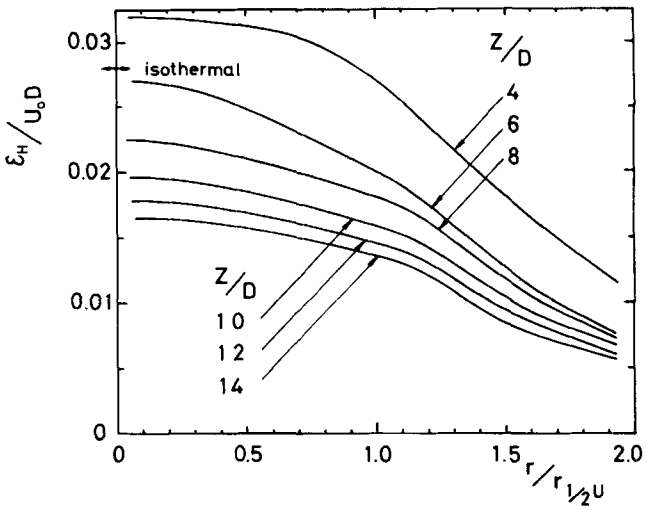

Fig. 10. Radial distribution of eddy diffusivity for heat.

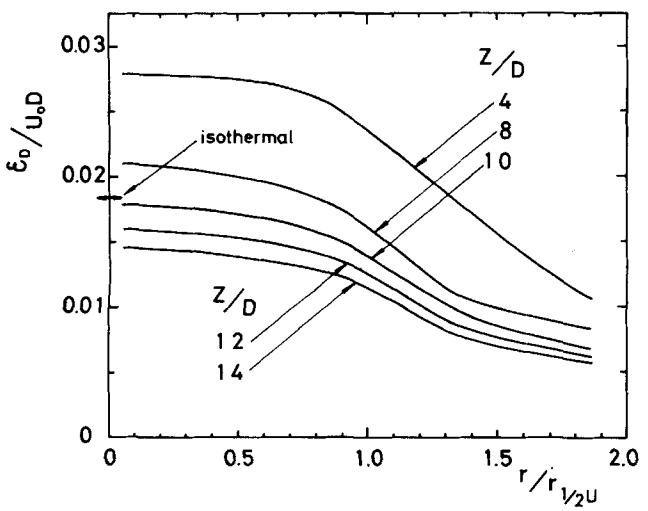

Fig. 11. Radial distribution of eddy diffusivity for mass.

isothermal jets obtained by a constant eddy diffusivity assumption (for example, Schlichting, 1955), and Equation (6) is the same in form as the Gaussian error curve which gives good agreement with the experimental distribution across the entire width of isothermal jets (for example, Hinze, 1959).

The transition region between the core and the fully developed region can be seen from Figures 7 and 8 to be very short. By comparison with the heated air into ambient air jet mixing data of Corrsin and Uberoi (1949), it is found that, as pointed out by Tomich and Weger (1967), the jet has more rapid jet spreading and center-line decay when the jet fluid is less dense than the receiving medium. It should be noted from Figure 7 that the decay rates of velocity and temperature are of the same order of magnitude, as distinct from Corrsin and Uberoi's data. Although Kiser's U decay curve (1963) is difficult to distinguish from Corrsin and Uberoi's T decay curve in Figure 7, the Kiser's water jet data seem to show a similar tendency between the velocity and concentration decays. The temperature half radius increases most rapidly with axial distance; the concentration half radius is, in turn, larger than the velocity half radius. This order of mixing is different from that of isothermal jet data given in the literature. These behaviors may suggest that static enthalpy instead of temperature should have been used as the thermal property of the high temperature jets.

According to Ricou and Spalding (1961), the jet spreading is related to the increase in the mass flow rate due to local entrainment, the rate of which is proportional to the square root of initial density ratio $\sqrt{\rho_\infty/\rho_o}$. Kleinstein (1964) and Wilson and Danckwerts (1964) showed the characteristic valuable for the streamwise coordinate to be $\sqrt{\rho_\infty/\rho_o}\,Z/D$.

The linear jet spreading and linear center-line decay obtained experimentally in the fully developed region can be expressed in terms of $\sqrt{\rho_\infty/\rho_o}\,Z/D$ as

$$\begin{cases} \dfrac{U_{\max}}{U_o} = 6.11\left(\sqrt{\dfrac{\rho_\infty}{\rho_o}}\dfrac{Z}{D} + 1.02\right)^{-1} \\ \dfrac{T_{\max}-T_\infty}{T_o-T_\infty} = 6.58\left(\sqrt{\dfrac{\rho_\infty}{\rho_o}}\dfrac{Z}{D} + 2.19\right)^{-1} \\ \dfrac{X_{\max}-X_\infty}{X_o-X_\infty} = 4.19\left(\sqrt{\dfrac{\rho_\infty}{\rho_o}}\dfrac{Z}{D} - 0.90\right)^{-1} \end{cases} \tag{7}$$

$$\begin{cases} \dfrac{r_{1/2U}}{D} = 0.0418\left(\sqrt{\dfrac{\rho_\infty}{\rho_o}}\dfrac{Z}{D} + 7.73\right) \\ \dfrac{r_{1/2T}}{D} = 0.0492\left(\sqrt{\dfrac{\rho_\infty}{\rho_o}}\dfrac{Z}{D} + 11.0\right) \\ \dfrac{r_{1/2X}}{D} = 0.0442\left(\sqrt{\dfrac{\rho_\infty}{\rho_o}}\dfrac{Z}{D} + 10.9\right) \end{cases} \tag{8}$$

These expressions are also similar in form to those of isothermal jet, except in that the effect of the initial density ratio is taken into account. Within the accuracy of the measurements, the proportionality constants in Equations (7) and (8), especially for the velocity data, agree well with the isothermal jet values obtained by many previous investigators (for example, Hinze and van der Hegge Zijnen, 1949; Kiser, 1963). Equation (7) gives a value of 5.09 for the core length $\sqrt{\rho_\infty/\rho_o}\,Z_c/D$ by substituting $U_{\max}/U_o = 1$ into the right-hand side, which agrees well with the Kleinstein's value of 4.73 within 10% error.

Since Equations (5) to (8) give all the radial profiles at any axial position in the fully developed region, these equations were used with the temperature dependent data of density and heat capacity to numerically integrate the right-hand side of Equation (4).

The local eddy diffusivities obtained are shown in Figures 9 to 11, where, for convenience of comparison, all the

radial coordinates were made dimensionless by using the velocity half radius. The small arrow located on the ordinate indicates the value for isothermal jet given in the literature.

According to Prandtl's mixing length hypothesis for isothermal jets exhausting into the still ambient medium, the eddy diffusivity for momentum is

$$\epsilon_M = K r_{1/2U} U_{\max} \tag{9}$$

For isothermal jets, $r_{1/2U}$ increases linearly, whereas $U_{\max}$ decreases linearly with axial distance. Hence, ϵ_M remains constant over the whole fully developed region, except in the outer, intermittent region.

However, it should be noted in Figures 9 to 11 that the observed eddy diffusivities for the highly heated jets in question decrease slightly with both the axial and the radial distances. For very low velocity, highly heated jets, this trend can be attributed to the change in volume of traveling eddies caused by the cooling process during the turbulent mixing with the cold ambient air. As aforementioned, a formulation of eddy diffusivities considering the volume change with temperature is more suitable as the representative coefficient of the turbulent, gradient transport model. According to Kleinstein's theory (1964), the dynamic eddy transfer coefficient is a constant, having the form

$$\frac{\rho \epsilon_M}{\rho_o U_o D} = \kappa \sqrt{\frac{\rho_\infty}{\rho_o}} \tag{10}$$

Figure 12 shows a result of the dimensionless dynamic eddy transfer coefficients calculated from the radial distribution of eddy diffusivities in Figures 9 to 11, where ρ and Cp are determined from the measured radial distribution of temperature.

These coefficients, as do the eddy diffusivities of isothermal jet, remain almost constant over the whole fully developed region of nonisothermal, heated jets except in the outer, intermittent region. The curve for $Z/D = 10$, which also lies between those for $Z/D = 8$ and 12, has been omitted to avoid the entangled diagram on the figure. Still, each coefficient has been found to decrease slightly but regularly with axial distance. It might suggest that, as Witze (1974) pointed out, there is still a little effect of the initial density ratio on the dynamic eddy transfer coefficients which were regarded to be constant by Kleinstein. In the present study, the proportionality constant κ was obtained by averaging the observed dynamic eddy transfer coefficients in the inner region over the range of axial distance $Z/D = 8$ to 12.

The resulting expressions are

$$\begin{cases} \dfrac{\rho \epsilon_M}{\rho_o U_o D} = 0.013 \sqrt{\dfrac{\rho_\infty}{\rho_o}} \\ \dfrac{\rho C p \epsilon_H}{\rho_o C p_o U_o D} = 0.019 \sqrt{\dfrac{\rho_\infty}{\rho_o}} \qquad (0 \leqq r/r_{1/2} \leqq 1) \\ \dfrac{\rho \epsilon_D}{\rho_o U_o D} = 0.019 \sqrt{\dfrac{\rho_\infty}{\rho_o}} \end{cases} \tag{11}$$

Although the coefficient for mass transfer seems to be slightly larger than that for energy transfer, both coefficients were regarded to have the same magnitude within the accuracy of the measurements. The proportionality constant κ for $\rho\epsilon_M$ was confirmed within maximum deviation of 30% by the supplementary experiments, although the experiments were performed in the relatively narrow range ($Re_o = 1\,600$, $\rho_\infty/\rho_o = 3.1$ to 5.1).

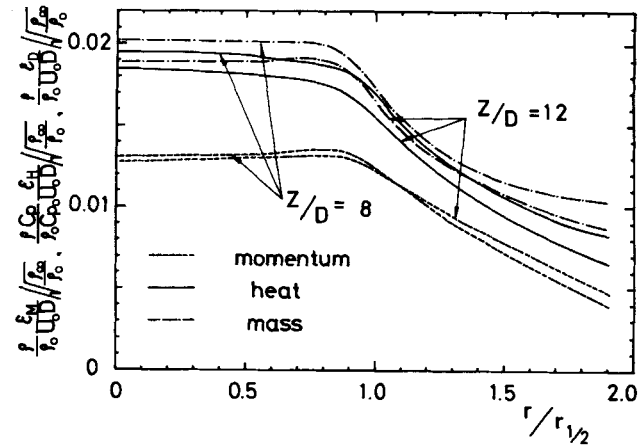

Fig. 12. Local dynamic eddy transfer coefficients calculated from the radial distribution of eddy diffusivities.

Warren's momentum transfer coefficient (1957), which was a linear function of the initial Mach number, did not explicitly take into account the change in density due to the temperature gradients in the flow field.

Kleinstein (1964) used Corrsin and Uberoi's heated air jet data (1949) ($\rho_\infty/\rho_o = 1$ to 2) to determine the empirical constant κ in his compressible model. The resulting expression for the dynamic eddy transfer coefficient is

$$\frac{\rho \epsilon_M}{\rho_o U_o D} = 0.00915 \sqrt{\frac{\rho_\infty}{\rho_o}} \tag{12}$$

Kleinstein's constant ($\kappa = 0.00915$) is slightly small compared with the present result ($\kappa = 0.013$). Tomich and Weger (1967) modified Kleinstein's model to apply in the core region as well as in the fully developed region. Witze (1974) considered the empirical constant κ as a function of the initial density ratio and the Mach number. Stowell and Smoot (1973) also gave similar empirical correlations. Still, much remains to be experimentally confirmed in the study of the turbulent transport mechanism for highly heated jets. Except for these models, only the unheated (or incompressible) jet experiments (ρ = constant) by other investigators are available for comparison with the present results.

Hinze and van der Hegge Zijnen (1949): slightly heated air jet

$$\begin{cases} \epsilon_M = 0.013\, U_o D \\ \epsilon_H = 0.018\, U_o D \end{cases} \tag{13}$$

Kiser (1963): submerged water jet with a sodium chloride tracer

$$\begin{cases} \epsilon_M = 0.0122\, U_o D \\ \epsilon_D = 0.0183\, U_o D \end{cases} \tag{14}$$

The mixing rate factor K in Equation (9) can be considered from the figure obtained by Donaldson and Gray (1966) to be 0.0233 for very low speed, isothermal jets issuing from a blunt edged nozzle. By using the isothermal jet mixing data on $r_{1/2U}$, $U_{\max}$ reported by many investigators, ϵ_M in Equation (9) can be readily estimated as

$$\epsilon_M = 0.0125\, U_o D \tag{15}$$

If ρ, Cp of Equation (11) are constant everywhere in the flow field (that is, $\rho = \rho_o = \rho_\infty$, $Cp = Cp_o$), Equation (11) becomes identical with Equations (13), (14), and (15). In other words, these isothermal relations are found to be a special form of Equation (11) in the case with constant ρ and Cp. Therefore, it can be considered that this dynamic eddy diffusion model [Equation (11)] is useful

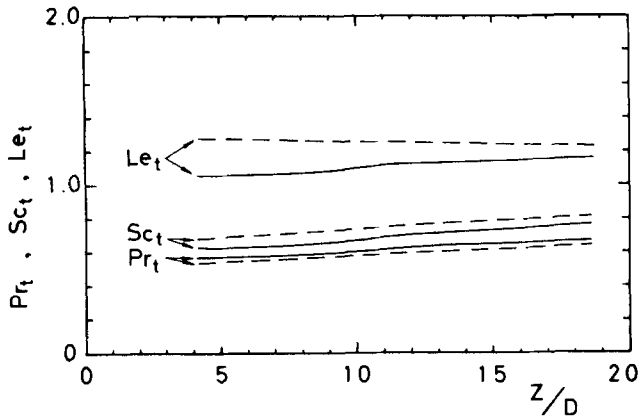

Fig. 13. Axial variation of turbulent Prandtl, Schmidt, and Lewis numbers. [The solid lines are based on the eddy diffusivity data in the inner region. The broken lines are obtained by substituting the measured half radii into Equation (16).]

in the fully developed region for both unheated (or incompressible) and heated jets at very low Mach numbers ($Ma \leqq$ about 0.1) over the wide range of the initial density ratio ($1 \leqq \rho_x/\rho_o \leqq 5.1$).

Figure 13 shows the axial variation of turbulent Prandtl, Schmidt, and Lewis numbers in the inner region, which were calculated by using the experimental values of eddy diffusivities in the inner region in Figures 9 to 11. As in the case of incompressible jets, these dimensionless values can also be calculated roughly from the experimental half radii with the aid of the following relations (for example, O'Connor et al., 1966):

$$\begin{cases} Pr_t = (r_{1/2U}/r_{1/2T})^2 \\ Sc_t = (r_{1/2U}/r_{1/2X})^2 \\ Le_t = Sc_t/Pr_t = (r_{1/2T}/r_{1/2X})^2 \end{cases} \tag{16}$$

Pr_t, Sc_t, and Le_t can be regarded to be roughly constant over the fully developed region. The turbulent Prandtl number is found to be about 0.6, slightly smaller than the Prandtl number for molecular transport of 0.68.

Finally, it should be noted again that the present model has been obtained experimentally in the fully developed region in the narrow ranges of the Reynolds number and the initial density ratio (that is, $1\,350 \leqq Re_o \leqq 1\,600$, $3.1 \leqq \rho_x/\rho_o \leqq 5.1$).

NOTATION

Cp = heat capacity at constant pressure
D = diameter of circular convergent nozzle
Ec = Eckert number
Gr = Grashof number
j = mass flux
K = mixing rate factor
l = mixing length
Le = Lewis number
M = molecular weight
Ma = Mach number
Pr = Prandtl number
q = heat flux
r = radial distance from jet axis
Re = Reynolds number
Sc = Schmidt number
T = temperature
U = axial velocity
V = volume of traveling eddy
v' = transverse component of turbulent velocity
X = concentration in mole fraction
y = distance in transverse direction
Z = axial distance from nozzle exit

Greek Letters

ΔT = temperature difference between the jet and the ambient
ϵ = eddy diffusivity
κ = empirical constant
ν = kinematic viscosity
ρ = density
τ = momentum flux

Subscripts

c = potential core
D = mass transport
H = heat transport
M = momentum transport
max = quantity on jet axis
o = quantity at nozzle exit
t = turbulent transport
1 = quantity of eddy 1
2 = quantity of eddy 2
1/2 = position within jet where property is one-half of center-line property
$1/2T$ = position where $T - T_\infty = (T_{\max} - T_\infty)/2$
$1/2U$ = position where $U = U_{\max}/2$
$1/2X$ = position where $X - X_\infty = (X_{\max} - X_\infty)/2$
∞ = quantity in the ambient surroundings

LITERATURE CITED

Corrsin, S., and M. S. Uberoi, "Further Experiments on the Flow and Heat Transfer in a Heated Turbulent Air Jet," *NACA TN 1865* (1949).

Donaldson, C. duP., and K. E. Gray, "Theoretical and Experimental Investigation of the Compressible Free Mixing of Two Dissimilar Gases," *AIAA J.*, **4**, No. 11, 2017 (1966).

Ferri, A., P. A. Libby, and V. Zakkay, "Theoretical and Experimental Investigation of Supersonic Combustion," *ARL 62-467*, Aeronautical Research Labs., Wright-Patterson Air Force Base, Ohio (Sept, 1962).

Hinze, J. O., *Turbulence*, McGraw-Hill, New York (1959).

———, and B. G. van der Hegge Zijnen, "Transfer of Heat and Matter in the Turbulent Mixing Zone of an Axially Symmetrical Jet," *Appl. Sci. Res.*, **1A**, 435 (1949).

Kiser, K. M., "Material and Momentum Transport in Axisymmetric Turbulent Jets of Water," *AIChE J.*, **9**, No. 3, 386 (1963).

Kleinstein, G., "Mixing in Turbulent Axially Symmetric Free Jets," *J. Spacecraft Rockets*, **1**, No. 4, 403 (1964).

O'Connor, T. J., E. H. Comfort, and L. A. Cass, "Turbulent Mixing of an Axisymmetric Jet of Partially Dissociated Nitrogen with Ambient Air," *AIAA J.*, **4**, No. 11, 2026 (1966).

Ricou, F. P., and D. B. Spalding, "Measurements of Entrainment by Axisymmetrical Turbulent Jets," *J. Fluid Mech.*, **11**, 21 (1961).

Schlichting, H., *Boundary-Layer Theory*, McGraw-Hill, New York (1955).

Stowell, D. E., and L. D. Smoot, "Turbulent Mixing Correlations in Free and Confined Jets," AIAA/SAE 9th Propulsion Conference, Las Vegas, Nev. (Nov., 1973).

Tomich, J. F., and E. Weger, "Some New Results on Momentum and Heat Transfer in Compressible Turbulent Free Jets," *AIChE J.*, **13**, No. 5, 948 (1967).

Warren, W. R., "An Analytical and Experimental Study of Compressible Free Jets," Ph.D. thesis, Princeton Univ., Princeton, N.J. (1957).

Wilson, R. A. M., and P. V. Danckwerts, "Studies in Turbulent Mixing—II. A Hot-Air Jet," *Chem. Eng. Sci.*, **19**, 885 (1964).

Witze, P. O., "Centerline Velocity Decay of Compressible Free Jets," *AIAA J.*, **12**, 417 (1974).

Manuscript received November 12, 1976; revision received July 22, and accepted August 4, 1977.